SCIENTIFIC REPORTS

OPEN

SUBJECT AREAS:
HIPPOCAMPUS
NEUROLOGICAL DISORDERS
HYPOXIA
DRUG DEVELOPMENT

Received
24 February 2014

Accepted
13 June 2014

Published
3 July 2014

Correspondence and requests for materials should be addressed to X.-T.W. (wangxt22@163.com)

* These authors contributed equally to this work.

Protective Effect of Dl-3n-butylphthalide on Learning and Memory Impairment Induced by Chronic Intermittent Hypoxia-Hypercapnia Exposure

Jing-jing Min[1,2]*, Xin-long Huo[1]*, ling-yun Xiang[1], Yan-qing Qin[1], Ke-qin Chai[1], Bin Wu[3], Lu Jin[1] & Xiao-tong Wang[1]

[1]The Center of Neurology and Rehabilitation, The Second Affiliated Hospital of Wenzhou Medical University, Wenzhou 325027, China, [2]The First People's Hospital of Huzhou, Huzhou 313000, China, [3]Wenzhou Medical University, Wenzhou 325027, China.

Cognitive impairment is a common finding in patients with chronic obstructive pulmonary disease (COPD), but little attention has been focused on therapeutic intervention for this complication. Chronic intermittent hypoxia hypercapnia (CIHH) exposure is considered to be responsible for the pathogenesis of COPD. Dl-3n-Butylphthalide (NBP), extracted from *Apium graveolens* Linn, has displayed a broad spectrum of neuroprotective properties. Our study aimed to investigate the potential of NBP on CIHH-induced cognitive deficits. The cognitive function of rats after CIHH exposure was evaluated by the Morris water maze, which showed that the NBP treated group performed better in the navigation test. NBP activated BDNF and phosphorylated CREB, the both are responsible for neuroprotection. Additionally, NBP decreased CIHH induced apoptosis. Moreover, NBP further induced the expression of HIF-1α, accompanied by the up-regulation of the autophagy proteins Bnip3, Beclin-1 and LC3-II. Finally, NBP also reversed the decreased expression of SIRT1 and PGC-1α, but the expression of Tfam, Cox II and mtDNA remained unchanged. These results suggested that the neuroprotective effects of NBP under CIHH condition possibly occurred through the inhibition of apoptosis, promotion of hypoxia-induced autophagy, and activation of the SIRT1/PGC-1α signalling pathway, while stimulation of mitochondrial biogenesis may not be a characteristic response.

Chronic obstructive pulmonary disease (COPD) is a debilitating disease characterised by incompletely reversible limitations in airflow. Airflow obstruction is the most common manifestation of COPD, but increasing reports have revealed its harmful effect on cognitive functions, which cannot be fully explained by coincidence or by depression[1]. Countless studies have indicated the association or causation between the suffering of hypoxia- hypercapnia and the progression of cognitive impairment in patients with COPD[2,3]. This phenomenon has aroused increasing attention, but still lacks appropriate treatment. The animal model of chronic intermittent hypoxia hypercapnia (CIHH) in our study mimicked the pathophysiological process in patients with COPD[4]. In our previous study, we confirmed that after 2 weeks of CIHH exposure, the learning and memory ability of the experimental rats deteriorated and became worse as the exposure time was lengthened[5,6].

Emerging studies suggest that neuronal apoptosis is a major contributor to hypoxia-induced cognitive lesions[7,8]. The Bcl-2 family members are major regulators of the intrinsic (mitochondrial) apoptotic pathway and act by shifting the balance between anti-apoptotic and pro-apoptotic members of the pathway[9]. Caspase-3, as the final executor of the caspase enzyme family, is indispensable for apoptotic chromatin condensation and DNA fragmentation[9].

Intracellular aggregation of altered and misfolded proteins is a common feature of most neurodegenerative disorders, such as Alzheimer's disease, Parkinson's disease or Huntington's disease[10]. Then, what goes wrong with these diseases? Increasing evidence highlights the role of autophagy in the clearance of these toxic products. Autophagy, which literally means "self-sacrificing", has been considered an active cell death pathway for decades. Only recently autophagy has been recognised as a cell survival pathway due to its irreplaceable role in degrading altered proteins and organelle turnover. However, many questions on the role of autophagy or the complicated interplay between apoptosis and autophagy are still debated. Regardless of the controversies, basal autophagy

plays a vital role in preventing the accumulation of abnormal organelles and proteins. Under stresses such as hypoxia or ischemia, defective autophagy or alterations in autophagy-related genes cause the accumulation of aggregated proteins and neurodegeneration, even in the absence of pathogenesis-related proteins[11,12]. Hypoxia-inducible factor 1α (HIF-1α) is an essential mediator of hypoxic signalling that regulates the transcription of hundreds of genes. Bcl-2/adenovirus E1B 19-kDa-interacting protein 3 (Bnip3), a member of the Bcl-2 pro-apoptotic family and a known HIF-1α target gene, has been shown to trigger autophagy under hypoxic conditions[13,14].

Mitochondria are highly dynamic organelles that produce adenosine triphosphate (ATP) for the excitability and survival of neurons. Compared with other regions, the neurons of the hippocampus have an intense demand for mitochondria and are more vulnerable to hypoxia[15]. SIRT1, a nicotinamide adenine dinucleotide (NAD^+)-dependent histone deacetylase, is activated by an increasing NAD+/NADH ratio. As a factor regulating longevity and DNA repair, SIRT1 can also deacetylate and activate PGC-1α[16,17]. PGC-1α co-activates transcription factors, including NRF-1 and NRF-2, for the promoters of mitochondrial transcription factor A (Tfam) to induce mitochondrial biogenesis and respiration. The biogenesis of mitochondria is a process that dynamically regulates the mitochondrial number and function under diverse pathophysiological conditions. SIRT1-mediated deacetylation and activation of PGC-1α also play protective roles against neurodegeneration[16,17].

Dl-3n-butylphthalide (NBP), a racemic mixture of an optical isomer, is extracted from the seeds of *Apium graveolens* Linn[18]. It is widely used for its therapeutic effects on ischemic strokes[19]. It has been shown to possess a range of pharmacological properties including anti-inflammatory, anti-vasospastic, anti-thrombic and anti-oxidative properties[20,21]. Additionally, NBP has also been shown to have neuroprotective effects against mitochondrial damage and anti-apoptosis in cerebral ischemia[22,23].

Presently, considerable efforts have been made to develop nootropics. Although some drugs such as memantine and acetylcholinesterase (AChE) inhibitors have been shown to ameliorate the symptoms of cognitive impairment in clinical studies, none of these drugs mediate the cognitive impairment process. A recent study indicated that in rats with vascular dementia, long-term treatment with NBP could attenuate the learning and memory deficits and promote angiogenesis, as well as increase the expression of growth factors, VEGF, the VEGF receptor and bFGF[24]. To the best of our knowledge, there is little data concerning the neuroprotective properties of NBP on CIHH-induced impaired cognitive function. In the current study, we attempted to determine whether chronic NBP administration could reverse CIHH-induced learning and memory deficits with a specific focus on apoptosis, hypoxia-induced autophagy and the SIRT1/PGC-1α signalling pathway. We hope to expand the understanding and provide new insights into the potential therapeutic value of NBP for neurodegenerative diseases.

Results

Chronic NBP treatment ameliorated spatial learning and memory ability in CIHH rats. After 2 weeks of CIHH exposure, rats displayed worse performances when locating a hidden platform, but this disruption was ameliorated by chronic NBP treatment (Fig. 1A). On the first and second days of training, each group demonstrated no significant difference in the escape latency time. However, from the third day forward, there were significantly ($p < 0.05$) prolonged latencies in the hypoxia-hypercapnia group (HH) and hypoxia-hypercapnia+ vegetable oil group (HY) compared with those of the normal control group (NC) (Fig. 1B). However, the rats subjected to NBP treatment showed a significant decrease in the latencies relative to HH group (Fig. 1B)($p < 0.05$). This similar tendency also appeared in the measurement of the distance moved, which showed a significant difference from the fourth day forward (Fig. 1C)($p < 0.05$). On the last day of the probe trial, each group showed no difference (Fig. 1D) ($p > 0.05$) which might be due to the small platform in a big pool.

Chronic NBP treatment promotes BDNF expression and CREB phosphorylation. To further confirm our findings from Morris water maze, we measured the cognition related proteins BDNF and CREB. Both are necessary components for the learning and memory formation processes. The BDNF and CREB expression were decreased after CIHH exposure, while treatment with NBP promoted BDNF expression and CREB phosphorylation (Fig. 2)($p < 0.05$).

Chronic NBP treatment decreased apoptotic cell death in CIHH rats. We examined the changes of the anti-apoptotic factor Bcl-2 and the pro-apoptotic factor Bax. Increasing expression of both Bcl-2 and Bax were present after 2 weeks of CIHH exposure as determined by Western blotting. NBP treatment substantially antagonised the increase in Bax, but further promoted Bcl-2 expression (Fig. 3A)($p < 0.05$). To confirm that the anti-apoptotic mechanism was indeed involved in the protective effect of NBP, we measured the expression of caspase-3 and the number of positive cells by the TUNEL assay. NBP administration counteracted the caspase-3 activation (Fig. 3A)($p < 0.05$). Consistent with down regulating apoptotic factors, TUNEL staining showed a decreased number of positive cells after NBP therapy (Fig. 3B)($p < 0.05$).

Chronic NBP treatment further induced HIF-1α-dependent autophagy in CIHH rats. Transmission electron microscopy showed that autophagosomes were present in the HH group and were evident in cells exposed to CIHH and treated with NBP (Fig. 4A). To molecularly confirm the induction of autophagy, we used Western blotting to measure the level of autophagy-related proteins. CIHH exposure induced an increase in Beclin-1 and the lipidated form of LC3(LC3-II), and both further improved after NBP administration (Fig. 4B) ($p < 0.01$). To unmask the precise mechanisms underlying the activation of autophagy, we further measured the alteration of HIF-1α,which has been implicated in hypoxia-induced autophagy as an adaptive metabolic response[14]. Western blotting and immunohistochemistry showed that the expression of HIF-1α was indeed improved under CIHH exposure and was further expressed after NBP administration (Fig. 4B and Fig. 4C) ($p < 0.05$), which was consistent with the expression of Bnip3, a known HIF-1α target protein (Fig. 3B) ($p < 0.05$). We speculated that the up-regulated Beclin-1 may be correlated with the increasing combination of Bnip3 and Bcl-2, which was confirmed by double immunofluorescence of the colocalisation of both Bnip3 and Bcl-2 (Fig. 5).

Chronic NBP treatment improved SIRT1 and PGC-1α expression, but showed no conclusive evidence for mitochondrial biogenesis. Increasing evidence has indicated that SIRT1 and PGC-1α may be neuroprotective and might be potential targets to treat neurodegenerative diseases[25,26]. In the presence of CIHH-induced cognitive lesions, there were significant decreases in relative protein levels of SIRT1 and PGC-1α (Fig. 6A) ($p < 0.05$), but levels of both proteins significantly increased in response to NBP treatment (Fig. 6A) ($p < 0.05$). Because PGC-1α often serves as a master regulator of mitochondrial biogenesis, we investigated the mitochondrial DNA (mtDNA) copy number by real-time PCR to determine whether mitochondrial biogenesis was involved. The results indicated decreasing mtDNA content under CIHH conditions (Fig. 6B) ($p < 0.05$) but no alteration after NBP exposure (Fig. 6B) ($p > 0.05$). To further substantiate this result, we observed Tfam and COX II expression at the translational level. Tfam is a direct regulator of mitochondrial DNA replication/transcription. COX II is one of the mitochondrial DNAs encoding protein which comprises the electron

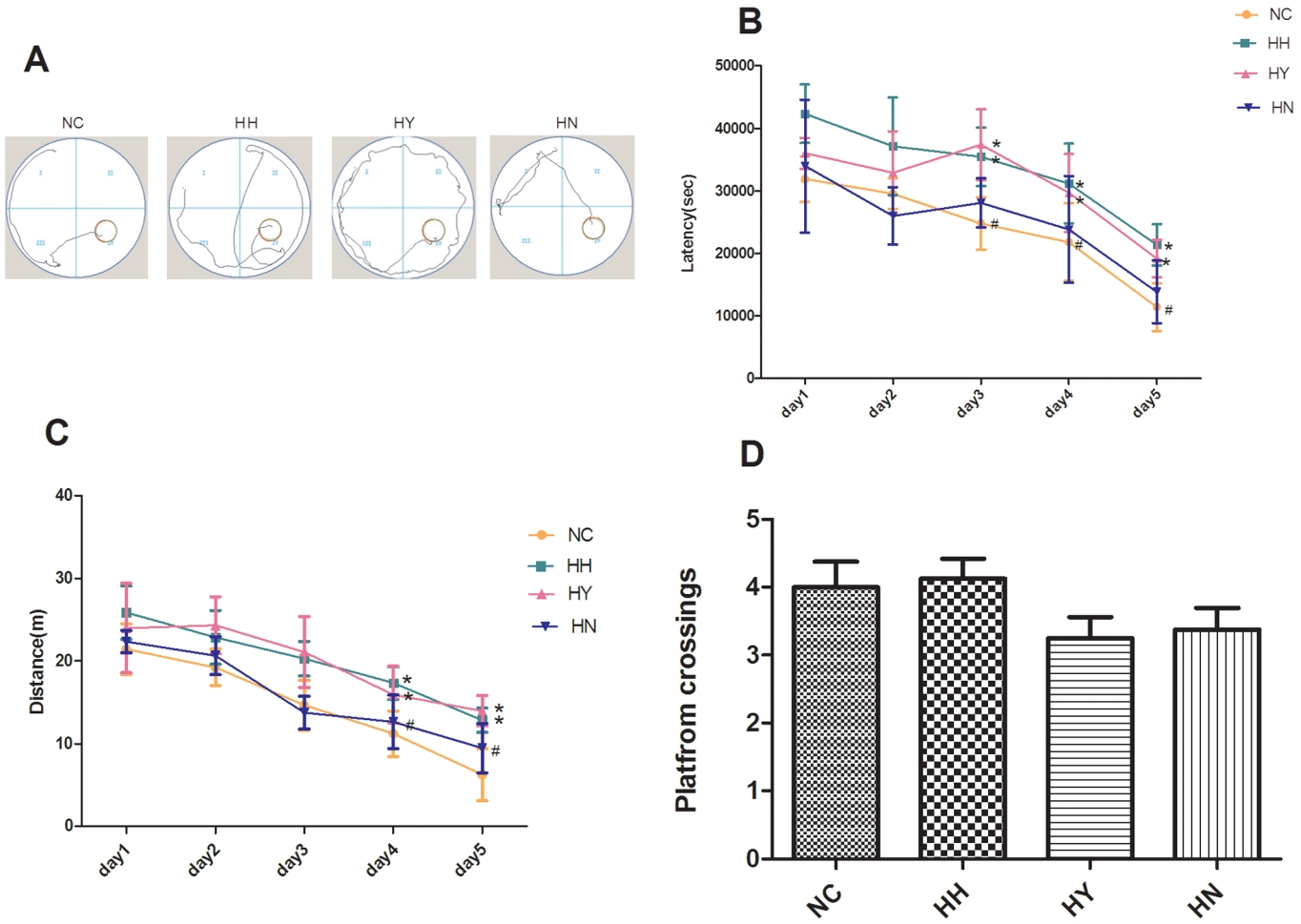

Figure 1 | NBP treatment improved the spatial learning and memory deficits in CIHH rats. (A) The pathway map to search for the hidden platform. (B) The mean escape latency time that the rats spent finding the hidden platform. (C) The distance moved to reach the hidden platform (D) The number of crossings of the location of the former platform. Values are expressed as the mean ± SEM. *P < 0.05 vs the NC group, #P < 0.05 vs the HH group. NC = normal control group; HH = hypoxia-hypercapnia group; HY = hypoxia-hypercapnia + vegetable oil group; HN = hypoxia-hypercapnia + NBP group.

transport chain. CIHH exposure down regulated the expression of both Tfam and COX II (Fig. 6B) ($p < 0.05$), but chronic NBP treatment was unable to change this reduction in expression (Fig. 6B) ($p > 0.05$).

Discussion

In the present study, we introduced the CIHH rat model to estimate the protective effects of NBP on cognitive function. Consistent with results from our previous study, behavioural data obtained from the

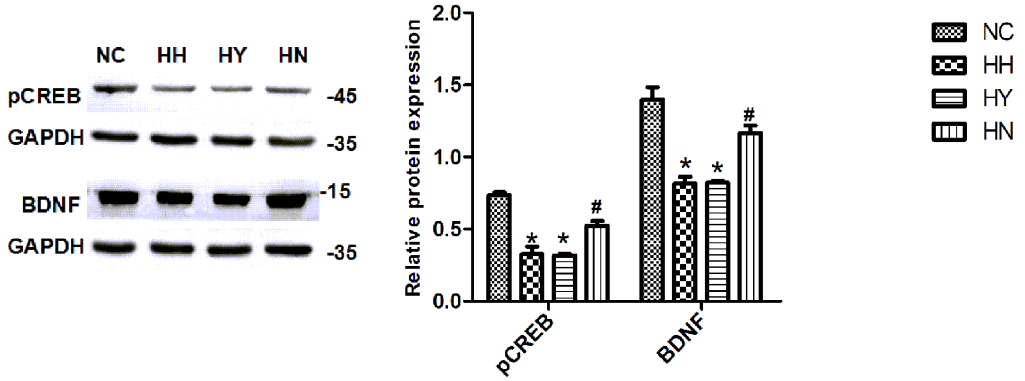

Figure 2 | Chronic NBP treatment promotes BDNF expression and CREB phosphorylation. Representative Western blots for BDNF and pCREB are shown. GAPDH was used as a loading control. The optical density values were normalised to their respective GAPDH loading control. The gels were run under the same experimental conditions, and cropped blots are used here. The full-length gel images are available in Supplementary Fig. 2. Values are expressed as the mean ± SEM. *P < 0.05 vs the NC group, #P < 0.05 vs the HH group. NC = normal control group; HH = hypoxia-hypercapnia group; HY = hypoxia-hypercapnia + vegetable oil group; HN = hypoxia-hypercapnia + NBP group.

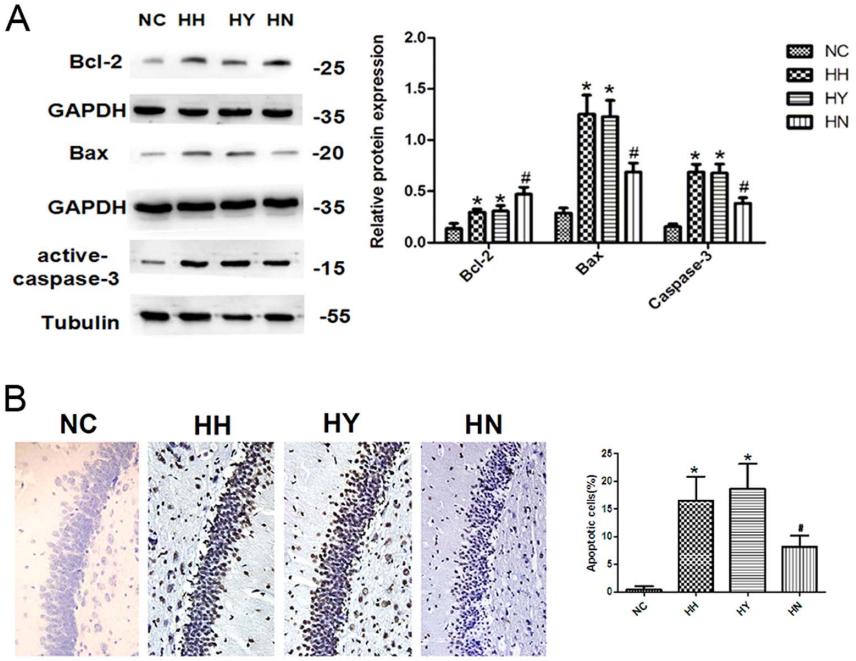

Figure 3 | NBP treatment decreased protein expression of the mitochondrial apoptotic factors and apoptotic cells. (A) The expression of Bcl-2, Bax and active-caspase-3 was determined by Western blotting. The optical density values were normalised to their respective GAPDH or Tubulin loading control. The gels have been run under the same experimental conditions, and cropped blots are used here. The full-length gel images are available in Supplementary Fig. 3A. (B) Apoptotic cells are stained by TUNEL (original magnification × 200). The bar graph shows the quantitative apoptotic cells obtained through the IPP analysis. Values are expressed as the mean ± SEM. *$P < 0.05$ vs the NC group, #$P < 0.05$ vs the HH group. NC = normal control group; HH = hypoxia-hypercapnia group; HY = hypoxia-hypercapnia + vegetable oil group; HN = hypoxia-hypercapnia + NBP group.

Morris water maze confirmed an obvious impairment on learning and memory performance in the CIHH rat model. However, chronic treatment with NBP possibly slowed CIHH-induced cognitive decline through attenuating mitochondrial apoptosis, promoting BDNF protein expression and CREB activation, as well as further improving the level of hypoxia-induced autophagy. We also provide evidence that SIRT1 induced deacetylation, and the resulting activation of PGC-1α may also be involved in the neuroprotective mechanism, but found no conspicuous evidence for mitochondrial biogenesis. Although our current study indicates the anti-apoptosis pathway is involved, the induction of hypoxia-induced autophagy and the activation of the SIRT1/PGC-1α signalling pathway also constitute important aspects of NBP action, we cannot rule out that NBP may interact with other biomolecules, in addition to those mentioned above, to exert its neuroprotective effects.

Brain-derived neurotrophic factor (BDNF) is one of the most prevalent neurotrophins that modulate synaptic activity[27]. The expression of BDNF is partially regulated by the transcription factor cAMP responsive element-binding (CREB), which represents a major integrator of signalling that influences neuronal plasticity and survival[27]. Learning and memory performance correlated well with the increases of BDNF and activation of CREB in the hippocampus. Our study indicated that NBP treatment increased the expression of BDNF and promoted the phosphorylation of CREB, which is consistent with the Morris water maze results.

Apoptosis is characterised by DNA fragmentation and an upregulation of pro-apoptotic proteins. It plays a pivotal role in oxygen deprivation induced cognitive impairment[28]. Because the Bcl-2 family members are located upstream of the irreversible cellular damage and focus most of their efforts on the level of the mitochondria, they are irreplaceable in deciding the fate of a cell. Bcl-2 is an anti-apoptotic protein that resides in the mitochondrial outer membrane. It normally forms a heterodimer with Bax to inhibit the activation of apoptosis. Bax, an anti-apoptotic pathway member, is primarily located in the cytosol in its inactive form. When apoptosis is triggered, Bax forms a homodimer with itself and translocates from the cytosol to the mitochondrial outer membrane[9]. Among the caspase family, caspase-3 is believed to be a hallmark of apoptotic cell death and acts as the final executor of apoptosis[29]. In our rat model, the expression of Bcl-2, Bax and caspase-3 all increased after CIHH stimulation. NBP intervention further induced Bcl-2 activity but significantly antagonised Bax and caspase-3 expression. Because DNA strand breaks occur during cell apoptosis, and the nicks in DNA molecules can be detected by the TUNEL assay[30], we also detected TUNEL-positive cells after CIHH stimulation. We observed that NBP treatment antagonised CIHH-induced increases in TUNEL-positive cells. These results support the idea that NBP is an effective anti-apoptotic reagent. Our results were in accordance with studies that showed that NBP reduced apoptosis and prevented mitochondrial damage in a focal cerebral ischemic or diabetic rat model[31,32].

Autophagy is characterised by the formation of double-membrane structures termed autophagosomes that can engulf cytoplasmic constituents into the lysosome/vacuole for degradation[33]. This process is essential for neuronal homeostasis and continuous remodelling of neuronal terminals[12]. Emerging evidence notes that defective autophagy leads to the accumulation of large, ubiquitin-containing inclusion bodies, which are the pathological hallmark of many neurodegenerative diseases[12]. Moreover, when cells are exposed to an unfavourable stimulus, such as hypoxia, autophagy will be rapidly activated or up-regulated as an adaptive response to promote cell survival[34]. On the other hand, recent elucidation of the predominant role of HIF-1α and its downstream target, Bnip3, in hypoxia-induced autophagy has greatly advanced our understanding of this process[35]. Bnip3, a known pro-apoptotic factor of the BH3-only Bcl-2 family, is gradually becoming recognised as capable of promoting protective autophagy-related genes, including Beclin-1 and Atg5, under oxygen deprivation[14]. Under such stress, the BH3-domain of Bnip3 can compete with Bcl-2 to dissociate the Bcl-2/Beclin-1 complex, releasing Beclin-1 from the complex and then triggering autophagy to

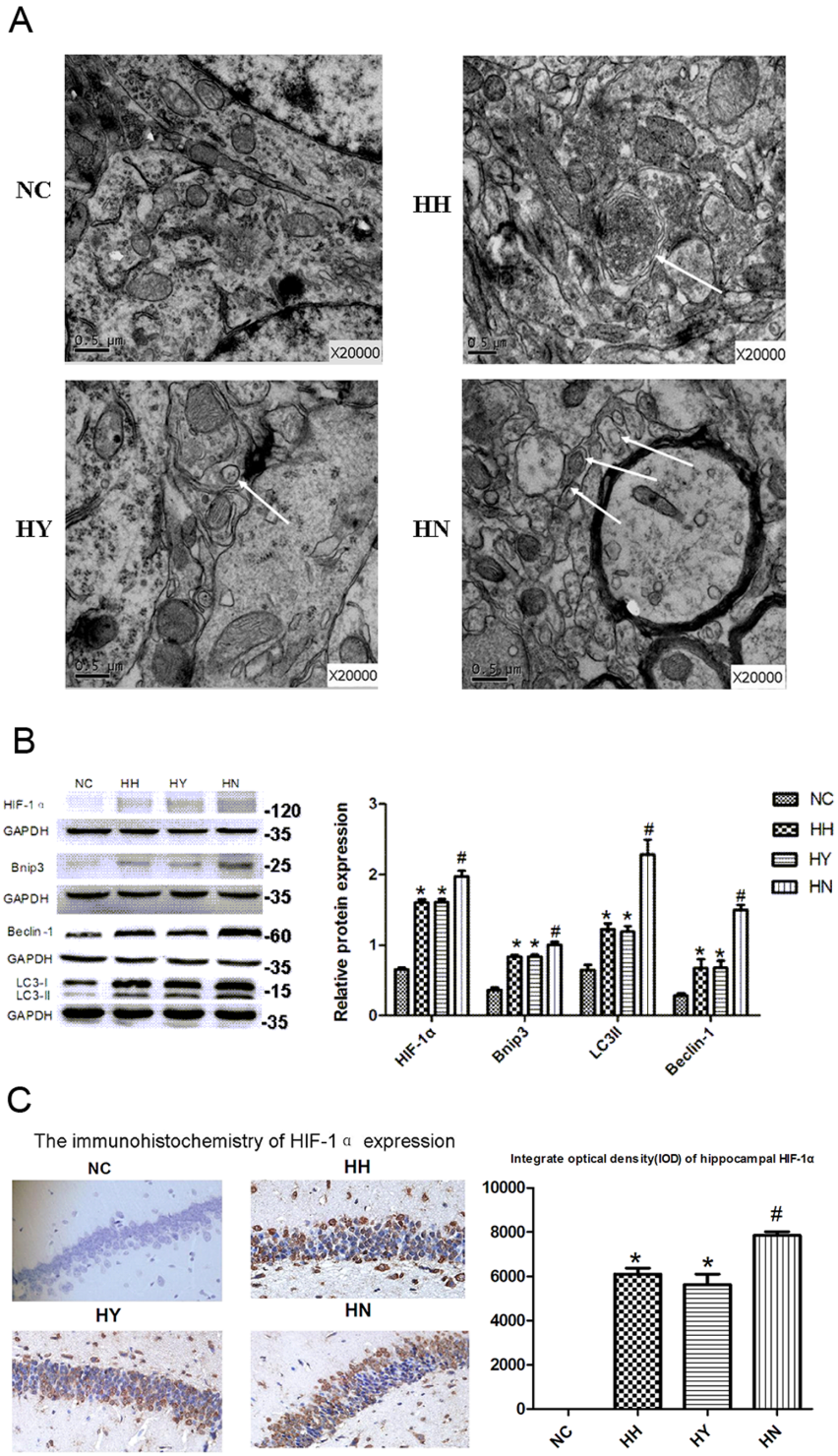

Figure 4 | NBP treatment further increased the level of hypoxia-induced autophagy. (A) Transmission electron microscopy shows the autophagosomes (white arrowheads), and the scale bars indicate 0.5 μm. (B) Representative western blots for HIF-1α, Bnip3, Beclin-1 and LC3 are shown. The optical density values were normalised to their respective GAPDH loading control. The gels have been run under the same experimental conditions, and cropped blots are used here. The full-length gel images are available in Supplementary Fig. 4B. (C) Photomicrographs showing hippocampal HIF-1α immunoreactivity (original magnification × 200). The bar graph showing the quantitative integrated optical density (IOD) obtained through the IPP analysis. Values are expressed as the mean ± SEM. *$P < 0.05$ vs the NC group, #$P < 0.05$ vs the HH group. NC = normal control group; HH = hypoxia-hypercapnia group; HY = hypoxia-hypercapnia + vegetable oil group; HN = hypoxia-hypercapnia + NBP group.

protect neurons from apoptosis[36]. These events may account for our immunofluorescence results that showed that the colocalisation of Bcl-2 and Bnip3 increased as autophagy was activated. Ectopic expression of both Bnip3 and Bnip3L (the Bnip3 homologue) are sufficient to initiate the autophagic process, even in the absence of oxygen and nutrient limitations, while the ablation of both under normoxic conditions promotes cell death[36,37]. Our current data showed that exposure to CIHH resulted in the induction of HIF-

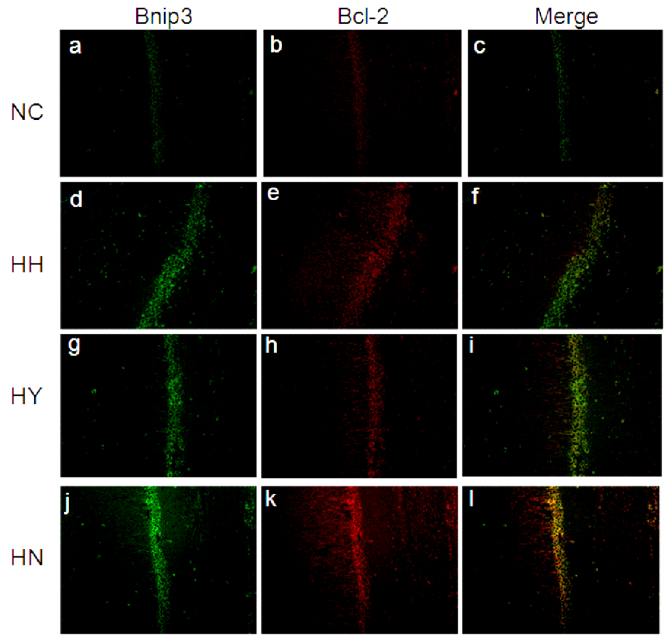

Figure 5 | NBP treatment made the colocalisation of Bnip3 and Bcl-2 evident. A digital photomicrograph under fluorescent illumination shows the colocalisation of Bnip3 and Bcl-2 (original magnification × 200). NC = normal control group; HH = hypoxia-hypercapnia group; HY = hypoxia-hypercapnia + vegetable oil group; HN = hypoxia-hypercapnia + NBP group.

1α, followed by activation of Bnip3. CIHH exposure also up-regulated the expression of Beclin-1 and LC3II, both used as markers of autophagy. Meanwhile, when the rats were treated with NBP, the autophagic markers and HIF-1α/Bnip3 expression were further induced and cognitive function was synchronously ameliorated. The altered proteins and damaged organelles produced by hypoxic-hypercapnic stress might be eliminated by this process, and further study is required to resolve this conjecture. The existence of cognitive impairment in NBP untreated groups might due to the fact that although hypoxia-induced autophagy played a protective role, the ongoing CIHH exposure continuously led to apoptosis and neuron reduction. In addition, the cognition related proteins such as pCREB and BDNF were also downregulated under CIHH conditions.

However, we cannot rule out the possibility that other oxygen-sensing pathways, in addition to HIF-1α/Bnip3 signalling, are also involved in hypoxia-induced autophagy. Due to the activation of the unfolded protein response (UPR), the inhibition of the mammalian target of rapamycin (mTOR) kinase signalling pathway and the activation of AMP-responsive protein kinase (AMPK) have been proposed to be related to the induction of autophagy[38–40]. Additionally, some novel factors have also been implicated in hypoxia-induced autophagy. Recently, Vasseur et al. demonstrated that the ablation of DJ-1, an oncogene regulating the transcription of the androgen-dependent receptor, impaired hypoxia-induced autophagy in U2OS cells[41]. In the meantime, Wilkinson et al. suggested that inhibition of the proteins of the PDGFR (platelet-derived growth factor receptor) family also block the hypoxia-induced autophagy in BE colorectal carcinoma cells[42]. Further studies are needed to determine whether other mechanisms also account for the effects of NBP on autophagy induction under CIHH conditions.

To survive in oxygen deprived environments, organisms must be capable of coping with redox imbalances and oxygen deficiencies. The NAD^+-dependent deacetylase SIRT1 plays a crucial role on the redox-sensing and oxygen-sensing pathways that mediate cell adaptation and longevity[43]. Meanwhile, both SIRT1-mediated deacetylation and activation of PGC-1α are important adaptive responses that increase mitochondrial metabolism. Previous studies on PGC-1α function in the brain were consistent with a primary role in neuroprotection[43,44]. PGC-1α knockout mice were hyperactive and displayed a progressive loss of striatal neurons, which were also primarily affected in Huntington's disease patients[45]. Intriguingly, in mice treated with resveratrol, the ectopic expression of SIRT1 also supported the neuroprotective role of SIRT1 in models for Alzheimer's disease and amyotrophic lateral sclerosis[26]. Considering the aforementioned findings, the SIRT1/PGC-1α pathway has been suggested as a neuroprotective axis for new therapeutic approaches to combat neurodegeneration[16]. On the other hand, PGC-1α is a "master regulator" of respiration and mitochondrial biogenesis. It can co-activate numerous transcription factors including NRFs to induce the promoter for Tfam, and Tfam can drive the transcription and replication of mitochondrial DNA (mtDNA)[46]. Mitochondrial DNA (mtDNA) encodes three cytochrome-*c* oxidase (COX) subunits (I−III) that regulate mitochondrial oxidative phosphorylation[47]. During hypoxia-hypercapnia exposure, the SIRT1/PGC-1α axis was inhibited, which might be due to the activation of CtBP (an inhibitor of SIRT1 transcription) or due to the NAD^+ diminution directly inactivating SIRT1. At the same time, Tfam and COX II protein expression and mtDNA gene expression provided direct indications of the suppression of mitochondrial biogenesis under the CIHH stimulus. After NBP exposure, although the expression of both SIRT1 and PGC-1α were improved, the amount of Tfam and COX II proteins and the mtDA copy number were not substantially changed. These divergent phenomena, especially the absence of any changes on mtDNA, are worth pondering. Several reasons may account for this separation. First of all, studies have found that PGC-1α also co-activates a large set of other genes termed oxidative phosphorylation (OXPHOS)-coregulated genes, as well as coordinates heme biosynthesis and triglyceride metabolism. So, the upregulation of PGC-1α may function separately from mitochondrial biogenesis[48]. Additionally, Tfam, which is unchanged after NBP exposure, is essential for the transcription, initiation and replication of mtDNA. It was previously reported that the transcription factors Sp1, NRF-1, NRF-2 were all critical for maintaining the transcription of the mammalian Tfam gene[48], and the DNA-free Tfam (Tfam unable to bind DNA) was prone to be degraded by the Lon protease[49]. Our current study did not focus on the regulation of Tfam, so further studies are still necessary. Moreover, increased hypoxia-induced autophagy may also suppress the increase of the mitochondrial content to lessen the energy expenditure[14]

In conclusion, the current study presents the functional role of NBP in ameliorating the learning and memory deficits caused by hypoxia-hypercapnia exposure. We propose that the possible mechanism involves inducing the cytoprotective function of hypoxia-induced autophagy and suppressing the level of apoptosis. NBP also activated the neuroprotective SIRT1/PGC-1α axis, but no evidence of mitochondrial biogenesis was found. Our study provides new insights into the long-term use of NBP as a potential treatment in early cognitive impairment caused by chronic obstructive pulmonary disease.

Methods

Animals and hypoxic exposure. Rat experiments were approved by the Ethics Committee of Wenzhou Medical University on the use of live animals in teaching and research (Approval no.wydy2012-0075). All experiments were performed in accordance with the relevant guidelines and regulations of the Laboratory Animal Unit of Wenzhou Medical University. Efforts were made to reduce the number of animals and to minimise their suffering. DL-3n-Butylphthalide (purity, 99.6%; lot number, 09100151) was obtained from Shijiazhuang Pharma Group NBP Pharmaceutical Co., Ltd (Shijiazhuang, Hebei, China). Six- to eight-week-old male Sprague-Dawley rats, weighing 180–220 g, were housed in the animal care facility with 12 h light/dark cycles and had free access to food and water. The rats were randomly divided into four groups: (i) normal control group (NC n = 16); (ii) hypoxia-hypercapnia group (HH n = 16); (iii) hypoxia-hypercapnia + vegetable oil group (HY n = 16) and (iv) hypoxia-hypercapnia + NBP (HN n = 16). The CIHH

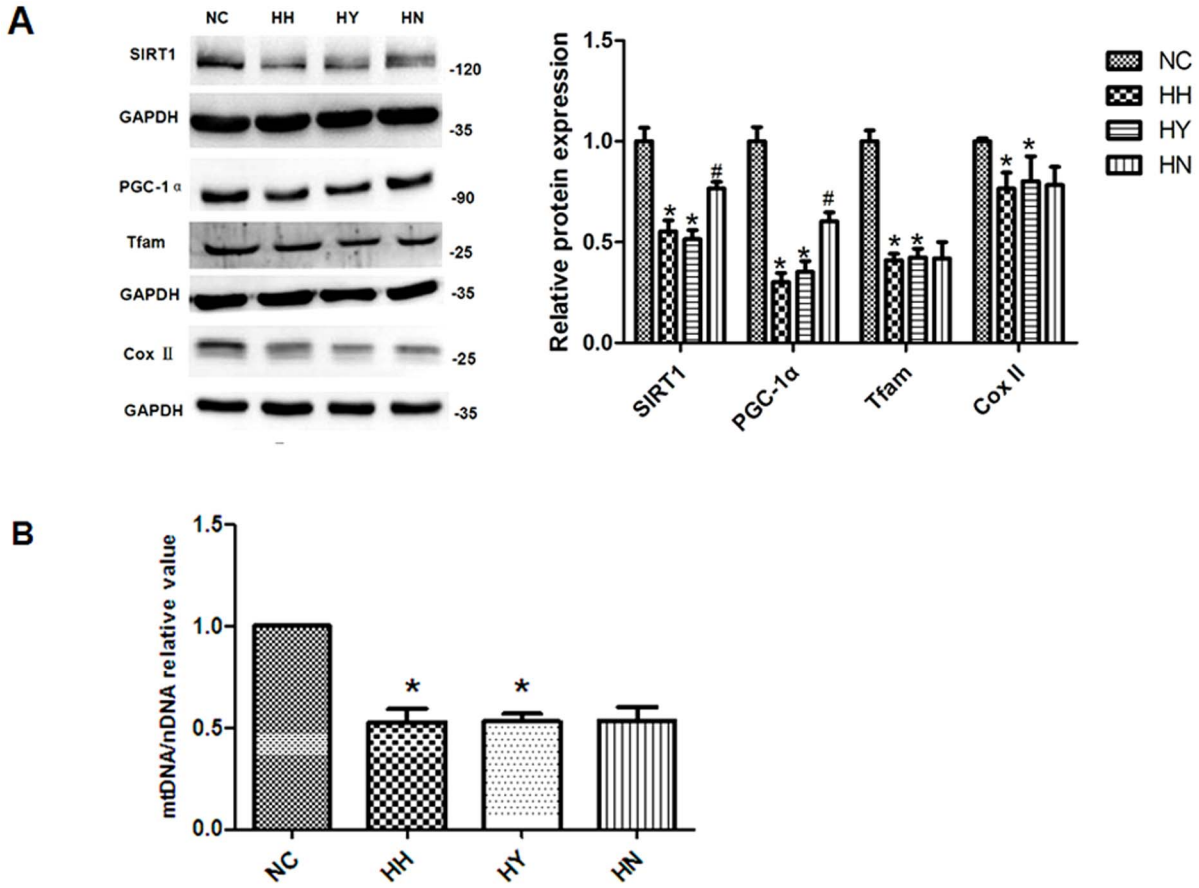

Figure 6 | NBP treatment improved the protein expression of Sirt1 and PGC-1α, but did not change Tfam and COX II expression or the mtDNA content. (A) Representative western blots for PGC-1α, Tfam and COX II are shown. GAPDH was used as a loading control. The optical density values were normalised to their respective GAPDH loading control. The gels have been run under the same experimental conditions, and cropped blots are used here. The full-length gel images are available in Supplementary Fig. 6A. (B) The mtDNA was corrected by the amount of nuclear DNA (β-actin). Values are expressed as the mean ± SEM *P < 0.05 vs the NC group, #P < 0.05 vs the HH group. NC = normal control group; HH = hypoxia-hypercapnia group; HY = hypoxia-hypercapnia + vegetable oil group; HN = hypoxia-hypercapnia + NBP group.

exposure was performed as previously described[5,6]. The rats in the latter three groups were intermittently placed in a closed chamber that was ventilated with an elevated CO_2 gas mixture (9%–11% O_2 + 6.5%–7.5%CO_2 in N_2) for 8 h/day, 6 days/week for 2 weeks. The conventional treatment of NBP is 10–12 days, and most studies use it as a chronic treatment. CIHH-induced cognitive impairment is a chronic and progressive neurodegenerative process. Therefore, dl-3n-Butylphthalide at a dose of 80 mg/kg or vegetable oil at the same dose was gavaged into the rat separately after the exposure cycle was completed each day for 2 weeks. The NBP dose applied here was determined from prior studies showing that this dose provided the maximal protective effects in the treatment of different brain diseases[50,51]. The NC group underwent identical handling and exposure, however, the chamber was flushed with room air instead of N_2.

The Morris water maze test. After the last hypoxia-hypercapnia exposure, the Morris water maze test was performed as previously described by Morris[52]. The Morris water maze sessions were conducted in a round tank, 1.5 m in diameter and 50 cm in deep, filled with water (35 cm depth). The water temperature was maintained at 26 ± 1°C. The pool was artificially divided into four imaginary quadrants. A 10-cm diameter platform was submerged 2 cm under the water surface in a fixed quadrant of the pool and could not be seen by the rats. During the experiments, the tank was videotaped by a video camera suspended above the maze, and the swimming paths, latency and distance moved to reach the escape platform were automatically recorded by an image analyser (SLY-WMS Morris Water Maze System; Sunny Instruments Co. Ltd., Beijing, China). The animals underwent 3 trials per day for 5 consecutive days. The rats were placed randomly into the pool, facing the wall, from four preset starting points, and they were allowed to swim for a maximum of 60 s. If the animal did not find the platform during a period of 60 s, it was gently guided to the platform and allowed to rest on it for 30 seconds. During the spatial probe trail, the platform was removed from the pool and the rats were allowed to swim for 60 s. The times of crossing the previous location of the platform was recorded.

Tissue preparation. After the Morris water maze test, the rats were deeply anesthetised by an intraperitoneal injection of 1.5 ml of 6% chloral hydrate and transcardially perfused with normal saline. The hippocampi from 8 rats of each group were rapidly removed and stored at −80°C for western blotting. The remaining rats were transcardially perfused with cold PBS followed by 4% paraformaldehyde in 0.1 M phosphate, pH 7.4. Two brains from each group were prepared for electron microscopy. The rest were prepared for TUNEL staining, immunofluorescence and immunohistochemistry.

Ultrastructure observations of the hippocampus with electron microscopy. The electron microscopy specimens were prepared as previously described[53]. The specimens were sectioned, prefixed in 2.5% glutaraldehyde for 4 h and postfixed with 1% osmium tetroxide at room temperature for 1 h, then embedded by epoxy resin 812 (Epon812). The grids were stained with 2% uranyl acetate (Merck, Germany), followed by lead citrate (Merck, Germany). The coronal ultra-thin sections of hippocampal CA1 regions were observed with a transmission electron microscope (Hitachi H-7500 electron, Japan).

Western blotting analysis. Equal amounts of the proteins (60 μg) were separated by SDS-polyacrylamide gels and transferred to polyvinylidene fluoride (PVDF) membranes (Millipore, Billerica, MA, USA). PVDF membranes were blocked for 2 h at room temperature with 5% fat-free powdered milk. Then, the membranes were incubated overnight at 4°C with respective primary antibodies including: anti-Bax, anti-active-Caspase-3, anti-Beclin-1, anti-LC3,anti-NRF-1, anti-COX II, and anti-pCREB antibodies, which were obtained from Cell Signalling Technology (Danvers, MA, USA); anti-BDNF, anti-Bnip3, anti-Bcl-2, anti-PGC-1α, anti-GAPDH and anti-Tubulin antibodies, which were obtained from Abcam (Cambridge, MA, USA); and anti-HIF-1α and anti-SIRT1 antibodies, from Novus Biologicals (Littleton, CO, USA). After incubation with the secondary goat-anti mouse or goat anti-rabbit antibody, the immunoreactive bands were detected by using BeyoECL Plus reagents.

Immunohistochemisrty. After dewaxing and hydration, the slides were incubated in citrate antigen-repairing solution and placed in a microwave oven at high power for 10 min. The solution was then allowed to cool at room temperature for 15 min, followed by washing in PBS for 5 min. To block the activity of endogenous

peroxidase, the slides were incubated in 3% hydrogen peroxide in methanol for 10 min at room temperature. To block the nonspecific binding, the slides were incubated with 5% normal goat serum in PBS for 30 min. After the step listed above, the slices were incubated with an anti-HIF-1α antibody (1 : 50, Novus Biologicals, USA) in PBS and then incubated with an HRP-conjugated secondary goat-anti mouse antibody (1 : 100, Abcam, UK) in PBS for 1 h. The slices were developed with DAB and counterstained with haematoxylin. The immunoreactive specificity was confirmed by omitting the primary antibody. The pyramidal cells in the CA1 region were examined.

Double Immunofluorescence Labelling. The sections were prepared in a conventional way, incubated in 0.1% sodium borohydride for 15 min to reduce the intensity of the autofluorescence from the paraffin and immersed for 30 min in a solution of 5% normal goat serum (Vector) in PBS. The sections were then incubated overnight with a mouse anti-Bnip3 antibody (diluted to 1 : 100 in PBS) and a rabbit anti-Bcl-2 antibody (diluted to 1 : 50 in PBS). This incubation was followed by three washes with PBST and incubation for 1 hour at room temperature in fluorescein isothiocyanate (FITC)-conjugated goat anti-mouse IgG (1 : 100) and Cy3- conjugated goat anti-rabbit IgG (1 : 100) antibodies. The sections were mounted and the pyramidal cells in the CA1 region were examined using an Olympus FluoView FV500 confocal microscope. The control sections were incubated with PBS instead of the primary antibodies.

TdT-mediated dUTP biotin nick end labelling (TUNEL). Double-strand DNA breaks were detected by the TUNEL assay. The deparaffinised sections were washed with distilled water and incubated with the Protein Digestion Enzyme for 20 min at 37°C. Then, we used the In Situ Cell Death Detection Kit (Roche Molecular Biochemicals) for the TUNEL assay according to the manufacturer's instructions. The pyramidal cells in the CA1 region were examined.

Determination of the mtDNA copy number. The mtDNA transcript levels were measured using the Roche LightCycler 480 real-time PCR system (Roche Co., Germany) with the SYBR Green detection method. The total hippocampal DNA was extracted using the QIAamp DNA mini kit (QIAGEN, Germantown, MD) according to the manufacturer's instructions. The relative mtDNA copy number was defined as the ratio of mtDNA (represented by the ND1 gene) to nuclear DNA (represented by the β-actin gene). The primers for the ND1 gene were ND1-forward, 5′-CCCTA-AAACCCGCCACATCT-3′ and ND1-reverse, 5′-GAGCGATGGTGAGAGCT-AAGGT-3′. The primers for the β-actin gene were β-actin-forward, 5′-TCACCAA-CTGGGACGATATG-3′ and β-actin-reverse, 5′-GTTGGCCTTAGGGTTCAGAG -3′. Each real-time PCR reaction (20 μl total volume) contained 2 μl of template DNA, 10 μl of SYBR Green Real-time PCR Master, 1 μl of each of the forward and reverse primers and 6 μl of ultrapure water. All data points were performed in triplicate.

Statistical Analysis. The Morris water maze latency and distance were analysed using repeated measures ANOVA (RM ANOVA). The other data were analysed by one-way ANOVA followed by a post hoc comparison test using the LSD (equal variances assumed) or Dunnett's T3 (equal variances not assumed) method. A value of $P < 0.05$ was considered to be statistically significant. The data were expressed as the mean ± SEM. All statistical procedures were performed with SPSS16.0 software.

1. Ortapamuk, H. & Naldoken, S. Brain perfusion abnormalities in chronic obstructive pulmonary disease: comparison with cognitive impairment. *Ann Nucl Med* **20**, 99–106 (2006).
2. Dodd, J., Getov, S. & Jones, P. Cognitive function in COPD. *Eur Respir J* **35**, 913–922 (2010).
3. Thakur, N. *et al.* COPD and cognitive impairment: the role of hypoxemia and oxygen therapy. *Int J Chron Obstruct Pulmon Dis* **5**, 263 (2010).
4. Zheng, G.-q., Wang, Y. & Wang, X.-t. Chronic hypoxia-hypercapnia influences cognitive function: A possible new model of cognitive dysfunction in chronic obstructive pulmonary disease. *Med Hypotheses* **71**, 111–113 (2008).
5. Wang, X.-t., Chen, S.-f. & Shao, S.-m. Effects of chronic hypoxic hypercapnia on cognition and expression of CREB in rats. *J Wenzhou Med Coll* **5**, 003 (2007).
6. Yang, X.-y. *et al.* Intervention of hydrogen on memory damage induced by chronic hypoxia-hypercapnia in rats. *Chinese J Pathophysiol* **3**, 029 (2011).
7. Niizuma, K. *et al.* Mitochondrial and apoptotic neuronal death signaling pathways in cerebral ischemia. *BBA-Mol Basis Dis* **1802**, 92–99 (2010).
8. Gozal, D. *et al.* Increased susceptibility to intermittent hypoxia in aging rats: changes in proteasomal activity, neuronal apoptosis and spatial function. *J Neurochem* **86**, 1545–1552 (2003).
9. Cheng, E. H.-Y. *et al.* BCL-2, BCL-X_L Sequester BH3 Domain-Only Molecules Preventing BAX-and BAK-Mediated Mitochondrial Apoptosis. *Mol cell* **8**, 705–711 (2001).
10. Ross, C. A. & Poirier, M. A. Protein aggregation and neurodegenerative disease. *Nat Med* **10**, 10–17 (2004).
11. Hara, T. *et al.* Suppression of basal autophagy in neural cells causes neurodegenerative disease in mice. *Nature* **441**, 885–889 (2006).
12. Komatsu, M. *et al.* Loss of autophagy in the central nervous system causes neurodegeneration in mice. *Nature* **441**, 880–884 (2006).
13. Hamacher, B. A. *et al.* Response to myocardial ischemia/reperfusion injury involves Bnip3 and autophagy. *Cell Death Differ* **14**, 146–157 (2006).
14. Zhang, H. *et al.* Mitochondrial autophagy is an HIF-1-dependent adaptive metabolic response to hypoxia. *J Bio Chem* **283**, 10892–10903 (2008).
15. Hota, S. K., Barhwal, K., Singh, S. B. & Ilavazhagan, G. Differential temporal response of hippocampus, cortex and cerebellum to hypobaric hypoxia: a biochemical approach. *Neurochem Int* **51**, 384–390 (2007).
16. Rasouri, S., Lagouge, M. & Auwerx, J. SIRT1/PGC-1: a neuroprotective axis? *M S-Med Sci* **23**, 840 (2007).
17. Jiang, M. *et al.* Neuroprotective role of Sirt1 in mammalian models of Huntington's disease through activation of multiple Sirt1 targets. *Nat Med* **18**, 153–158 (2011).
18. Liu, C.-L. *et al.* Dl-3n-butylphthalide prevents stroke via improvement of cerebral microvessels in RHRSP. *J Neurol Sci* **260**, 106–113 (2007).
19. Zhang, L. *et al.* Effects of Dl-3-n-butylphthalide on vascular dementia and angiogenesis. *Neuroche Res* **37**, 911–919 (2012).
20. Peng, Y., Zeng, X., Feng, Y. & Wang, X. Antiplatelet and antithrombotic activity of L-3-n-butylphthalide in rats. *J Cardiovasc Pharm* **43**, 876–881 (2004).
21. Hao, L.-X. & Yi, P.-F. Inhibitory effects of chiral 3-n-butylphthalide on inflammation following focal ischemic brain injury in rats. *Acta Pharmacol Sin* **21**, 433–438 (1999).
22. Chang, Q. & Wang, X. L. Effects Of Chiral 3-n-butylphthalide On Neuronal Apoptosis Induced By Transient Focal Cerebral Ischemia In Rats. *Inte J Pharm* **1** (2002).
23. Xiong, J. & Feng, Y. The protective effect of butylphthalide against mitochondrial injury during cerebral ischemia. *Acta Pharmacol Sin* **35**, 408–412 (2000).
24. Zhang, Li. *et al.* Effects of Dl-3-n-butylphthalide on vascular dementia and angiogenesis. *Neurochem Res* **37**, 911–919 (2012).
25. Brunet, A. *et al.* Stress-dependent regulation of FOXO transcription factors by the SIRT1 deacetylase. *Science* **303**, 2011–2015 (2004).
26. Kim, D. *et al.* SIRT1 deacetylase protects against neurodegeneration in models for Alzheimer's disease and amyotrophic lateral sclerosis. *EMBO J* **26**, 3169–3179 (2007).
27. Aso, E. *et al.* BDNF impairment in the hippocampus is related to enhanced despair behavior in CB1 knockout mice. *J Neurochem* 2008, **105**(2): 565–572.
28. Friedlander, R. M. Apoptosis and caspases in neurodegenerative diseases. *N Engl J Med* **348**, 1365–1375 (2003).
29. Degterev, A., Boyce, M. & Yuan, J. A decade of caspases. *Oncogene* **22**, 8543–8567 (2003).
30. Charriaut-Marlangue, C. & Ben-Ari, Y. A cautionary note on the use of the TUNEL stain to determine apoptosis. *Neuroreport* **7**, 61–64 (1995).
31. Li, J. *et al.* dl-3n-Butylphthalide prevents neuronal cell death after focal cerebral ischemia in mice via the JNK pathway. *Brain Res* **1359**, 216–226 (2010).
32. Zhang, T., Jia, W. & Sun, X. 3-n-Butylphthalide (NBP) reduces apoptosis and enhances vascular endothelial growth factor (VEGF) up-regulation in diabetic rats. *Neurol Res* **32**, 390–396 (2010).
33. Yang, Y., Xing, D., Zhou, F. & Chen, Q. Mitochondrial autophagy protects against heat shock-induced apoptosis through reducing cytosolic cytochrome *c* release and downstream caspase-3 activation. *Biochem Bioph Res Co* **395**, 190–195 (2010).
34. Levine, B. & Kroemer, G. Autophagy in the pathogenesis of disease. *Cell* **132**, 27–42 (2008).
35. Azad, M. B. *et al.* Hypoxia induces autophagic cell death in apoptosis-competent cells through a mechanism involving BNIP3. *Autophagy* **4**, 195–204 (2008).
36. Bellot, G. *et al.* Hypoxia-induced autophagy is mediated through hypoxia-inducible factor induction of BNIP3 and BNIP3L via their BH3 domains. *Mol Cell Biol* **29**, 2570–2581 (2009).
37. Mazure, N. M. & Pouysségur, J. Atypical BH3-domains of BNIP3 and BNIP3L lead to autophagy in hypoxia. *Autophagy* **5**, 868–869 (2009).
38. Papandreou, I., Lim, A. L., Laderoute, K. & Denko, N. C. Hypoxia signals autophagy in tumor cells via AMPK activity, independent of HIF-1, BNIP3, and BNIP3L. *Cell Death Differ* **15**, 1572–1581 (2008).
39. Pouysségur, J., Dayan, F. & Mazure, N. M. Hypoxia signalling in cancer and approaches to enforce tumour regression. *Nature* **441**, 437–443 (2006).
40. Rouschop, K. M. *et al.* The unfolded protein response protects human tumor cells during hypoxia through regulation of the autophagy genes MAP1LC3B and ATG5. *J Clin Invest* **120**, 127–141 (2010).
41. Vasseur, S. *et al.* DJ-1/PARK7 is an important mediator of hypoxia-induced cellular responses. *P Natl Acad Sci* **106**, 1111–1116 (2009).
42. Wilkinson, S., O'Prey, J., Fricker, M. & Ryan, K. M. Hypoxia-selective macroautophagy and cell survival signaled by autocrine PDGFR activity. *Genes Dev* **23**, 1283–1288 (2009).
43. Rodgers, J. T., Lerin, C., Gerhart-Hines, Z. & Puigserver, P. Metabolic adaptations through the PGC-1α and SIRT1 pathways. *FEBS Lett* **582**, 46–53 (2008).
44. Cui, L. *et al.* Transcriptional repression of PGC-1α by mutant huntingtin leads to mitochondrial dysfunction and neurodegeneration. *Cell* **127**, 59–69 (2006).
45. Lin, J. *et al.* Defects in Adaptive Energy Metabolism with CNS-Linked Hyperactivity in< i> PGC-1α Null Mice. *Cell* **119**, 121–135 (2004).
46. Lin, J., Handschin, C. & Spiegelman, B. M. Metabolic control through the PGC-1 family of transcription coactivators. *Cell Metab* **1**, 361–370 (2005).
47. Papadopoulou, L. C. *et al.* Fatal infantile cardioencephalomyopathy with COX deficiency and mutations in SCO2, a COX assembly gene. *Nat Genet* **23**, 333–337 (1999).

48. Matsushima, Y., Goto, Y. & Kaguni, L. S. Mitochondrial Lon protease regulates mitochondrial DNA copy number and transcription by selective degradation of mitochondrial transcription factor A (TFAM). *Proc Natl Acad Sci USA* **107**, 18410–5 (2010).
49. Dong, X. *et al*. Mitochondrial transcription factor A and its downstream targets are up-regulated in a rat hepatoma. *J Biol Chem* **277**, 43309–43318 (2002).
50. Liu, X.-G. & Feng, Y.-P. Protective effect of dl-3-n-butylphthalide on ischemic neurological damage and abnormal behavior in rats subjected to focal ischemia. *Acta Pharmacol Sin* **1995**, 30(12): 896–903.
51. Liao, S. *et al*. Enhanced angiogenesis with dl-3n-butylphthalide treatment after focal cerebral ischemia in RHRSP. *Brain Res* **1289**, 69–78 (2009).
52. Morris, R. Developments of a water-maze procedure for studying spatial learning in the rat. *J Neurosci Meth* **11**, 47–60 (1984).
53. Cai, X.-H. *et al*. Chronic intermittent hypoxia exposure induces memory impairment in growing rats. *Acta Neurobiol Exp* **70**, 279–287 (2010).

Acknowledgments

We thank Dr Jiangfan Chen, Department of Neurology, Boston University School of Medicine, Boston, for the critical review and preparation of the manuscript. This research was supported by the Medical Science Research Foundation of Zhejiang Province grant (NO: Y205233) and by Wenzhou City Science and Technology Bureau grant (NO:Y2005A001). No author or related institution has received any financial benefit from research in this study.

Author contributions

The work presented here was carried out in collaboration between all authors.Conceived and designed the experiments: J.J.M., X.L.H., X.T.W. Performed the experiments: J.J.M., X.L.H. Analyzed the data: L.Y.X., K.Q.C. Contributed reagents/materials/analysis tools: Y.Q.Q., L.J., B.W. Wrote the paper:J.J.M., X.L.H., X.T.W.

Additional information

Supplementary information accompanies this paper at http://www.nature.com/scientificreports

Competing financial interests: The authors declare no competing financial interests.

How to cite this article: Min, J.-j. *et al*. Protective Effect of Dl-3n-butylphthalide on Learning and Memory Impairment Induced by Chronic Intermittent Hypoxia-Hypercapnia Exposure. *Sci. Rep.* **4**, 5555; DOI:10.1038/srep05555 (2014).